FAULT ANALYSIS ON A NAVAL POWER GRID USING EQUIVALENT IMPEDANCES

By:

K.R. Davey

1st WSEAS International Conference on Electroscience and Technology for Naval Engineering and All-Electric Ship, Athens, Greece, July 12-13, 2004

IASME Transactions, vol. 1, no. 2, April 2004, pp. 247-251

PR - 363

Center for Electromechanics
The University of Texas at Austin
PRC, Mail Code R7000
Austin, TX 78712
(512) 471-4496

April 23, 2004

Fault Analysis on a Naval Power Grid using Equivalent Impedances

KENT DAVEY
Center for Electromechanics
The University of Texas at Austin
1 University Station R7000, Austin, Texas, 78759
UNITED STATES OF AMERICA
k.davey@mail.utexas.edu, http://www.utexas.edu/research/cem/

Abstract - The electrical system on a ship is well contained. Among the challenges proffered by naval systems is real time monitoring for the purpose of fault analysis and reconfiguration. The system can be considered as a grid of interconnected or terminated trunk lines, each with its own equivalent parallel load impedance and series transmission impedance. An algorithm is presented for predicting these equivalent impedances in subcycle intervals even through a transient. A precipitous drop in the magnitude of a load impedance earmarks the onset of a fault. The sensitivity of this approach to measured signal to noise ratio is investigated. Examples are shown to demonstrate how the magnitude and phase of equivalent load impedances change through unbalanced faults.

Key Words – impedance, phasor, transient, fault, detection

1 Introduction

The conventional approach for managing faults has been to use differential relays, and they have proved to be quite reliable. The main disadvantage is the hardware and setup required for initial balancing. One differential relay is required for each zone of protection required; the relay protects against a fault within its zone. Advances in measurement techniques and primarily computing power have prompted research into new ways to detect faults.

Jiao proposes a combination of three phase negative sequences to construct a synthetic negative sequence vector, which might be used to detect earth faults during power swings [1]. During the fault, the negative sequence current is much smaller than the zero sequence component, and is therefore suggested as guide indicator [2]. Styvaktakis recommends looking only at line voltage dip through a Kalman filter, but warns that events other than fault induced dips would also trigger this indicator [3]. Qianlisuggests an index based on the maximum of the wavelet transformation of current with different scales [4]. However the fault phase is determined only by matching these characteristics to faults of different types.

Wiot shares a view with these authors, i.e., that that fault inceptions and switching events occurring in the vicinity of the protective relay can be detected by monitoring voltages and currents [5]. His method is based on a least-square minimization of the residual signal given by a short Fourier filter with two adapted coefficients. The method proposed in this paper is believed to be more straightforward and involves directly computing the magnitude and phase of any signal based on three consecutive measurements. During a transient, either the frequency or phase can be treated as a variable parameter. Phase variation is assumed in this paper. 2 Real Time to Phasor Conversion

The sampling of current and voltage in time periods much shorter than the fundamental period is not useful by itself. In a time harmonic system with primary frequency ω, key parameters such as current and voltage can be represented over a short period of time with a magnitude and a phase. The ratio of the magnitudes and the difference of the phases is the key to rapid detection of faults. The currents on the phase A and B lines can be written as

$$I_A = A\cos(\omega t) \tag{1}$$

$$I_B = B\cos(\omega t - \phi) \tag{2}$$

The hypothesis posited in this paper is that magnitude and phase of equivalent impedances offer the possibility of fault identification in sub-

cycle time periods. The magnitude itself can be expressed as a sinusoid or a sum of sinusoids with frequencies different from ω. The product of two sinusoids with different frequencies is equivalent to another sinusoid with a different frequency. This approach will handle the fact that the frequency is not really constant during a transient. Suppose the currents are being sampled with Hall effect probes at time interval δt. Define the signals s_1 through s_6 as

$$\begin{aligned} s_1 &= A\cos(\omega t) \\ s_2 &= A\cos(\omega(t+\delta t)) \\ s_3 &= A\cos(\omega(t+2\delta t)) \\ s_4 &= B\cos(\omega t-\phi) \\ s_5 &= B\cos(\omega(t+\delta t)-\phi) \\ s_6 &= B\cos(\omega(t+2\delta t)-\phi) \end{aligned} \qquad 3)$$

Observe that

$$\frac{A}{B}=\frac{s_1\cos(\phi)\,s_2\cos(\omega\delta t-\phi)}{s_4+s_5\cos(\omega\delta t)} \qquad (4)$$

The assumption of phase 0 for signal s_1 is not a limitation because t is an arbitrary number. This expression is interesting but not very useful unless the phase is known a priori. The problem is that the time is unknown and the sampling period is short. Consider rearranging this into three equations,

$$\begin{aligned} s_1\cos(\omega t-\phi) &= \frac{A}{B}s_4\cos(\omega t) \\ s_2\cos(\omega(t+2\delta t)-\phi) &= \frac{A}{B}s_5(\cos(\omega(t+\delta t))) \\ s_3\cos(\omega(t+2\delta t)-\phi) &= \frac{A}{B}s_6(\cos(\omega(t+2\delta t))) \end{aligned} \qquad (5)$$

There are three unknowns, time t, which is of no concern, the phase ϕ, and the magnitude ratio A/B. These equations can be solved analytically to determine the magnitude ratios and the relative phase.

Shown in Fig. 1 is the predicted percent error in the prediction of A/B with only three sample points separated in time by the number of milliseconds marked on the abscissa. A 5% random noise signal was added to the measurement of each signal, s_1 through s_6. In this test, the peak errors can never be expected to be lower than twice the noise signal. As shown below, this can be achieved if the signal is over-sampled, i.e., if there is a minimum of 4 data points.

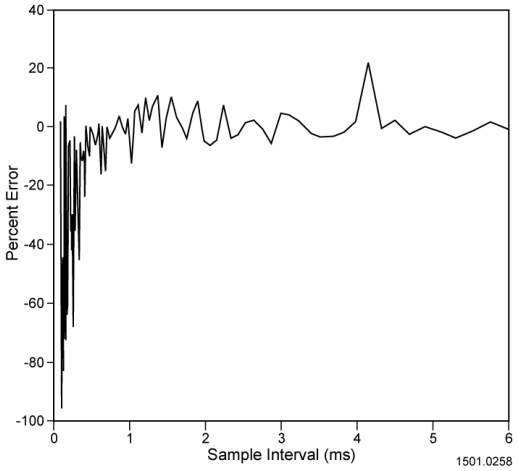

Fig. 1. Percent error as a function of sample time with a 5% noise signal added to each reading

When the measurement noise is reduced to 2%, the error in the prediction changes to that shown in Fig. 2. These plots suggest that fault detection might conceivably be done reliably in 2-3 ms, allowing a δt of about 1 ms. Phase is not as sensitive to noise. Shown in Fig. 3 is the phase prediction with a 5% random noise signal added to the measured signals. The results support the supposition that accurate system assessment can be determined from subcycle waveform sampling.

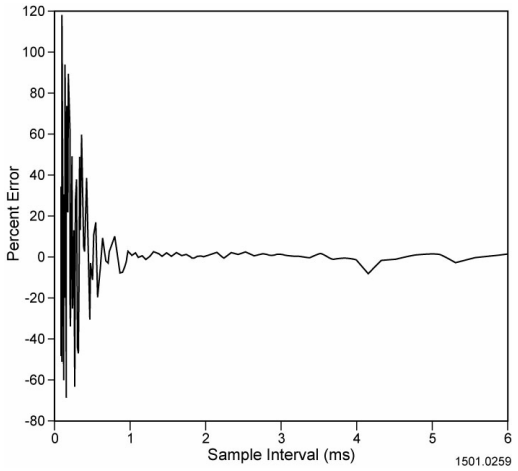

Fig. 2. Percent error when 2% noise is added to each sample reading

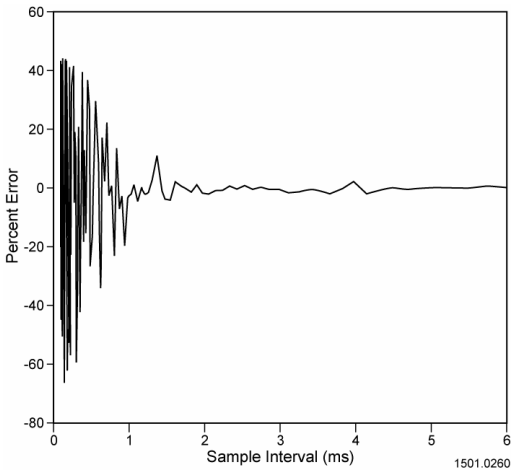

Fig. 3. Phase error when 5% random noise is added to the measured signals

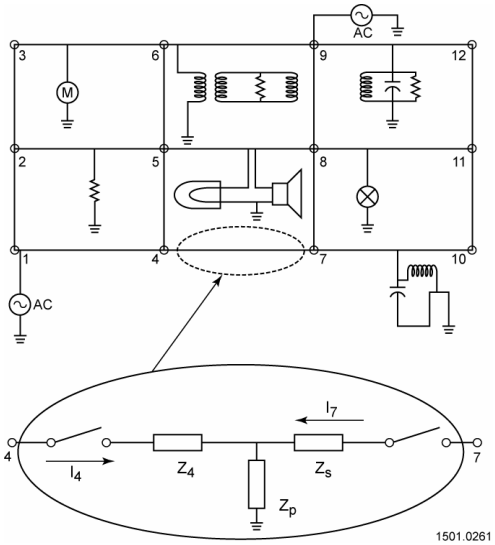

Fig. 4. Power circuit grid layout using designated trunk lines

3 Equivalent Circuit Representation and Fault Control

Power grids can be laid out using trunk lines and loads to ground from these lines as depicted in Fig. 4. Every trunk line has isolation switches on both ends, and sensors measuring voltage and current leaving their respective nodes. Multiple loads are connected to any one trunk line. Although the load is variable, this load can be represented by a series impedance Z_s on both sides of a parallel impedance Z_p. The choice of an equal impedance on both sides of the parallel load is an arbitrary choice, and it will not affect load flow calculations.

These impedances are determined from the measurements for voltage and current. Using the results of the previous section and noting that the voltages and current are to be understood as phasor quantities, the impedances for the 4-7 trunk line annotated in the figure inset would follow as

$$Z_s = \frac{2(V_4 - V_7)}{(I_4 - I_7)} \tag{6}$$

$$Z_p = \frac{(V_7 I_4 - V_4 I_7)}{I_4^2 - I_7^2} \tag{7}$$

The procedure outlined in equation (5) is a technique for determining the relative magnitude and phase between any two signals. Of interest is the magnitude and phase of Z_s and Z_p between any two nodes i and j. Equation (5) must be repeated three times to get Z_s since the general formula

$$Z_{sij} = 2\frac{V_i}{I_i}\frac{\left(1 - \frac{V_j}{V_i}\right)}{\left(1 - \frac{I_j}{I_i}\right)} \tag{8}$$

depends on the relative magnitude and phase between V_i and I_i, V_j and V_i, and I_j and I_i. A fourth relative and magnitude and phase is required to get Z_p, that between V_j and I_i,

$$Z_{pij} = \frac{\left(\frac{V_j}{I_i} - \frac{V_i}{I_i}\cdot\frac{I_j}{I_i}\right)}{\left(1 - \left(\frac{I_j}{I_i}\right)^2\right)} \tag{9}$$

Because equations (8) and (9) are updated in real time, these quantities are dynamic. These two impedances adequately represent even the most nonlinear system for short time periods, and they are the key to fault control. Each trunk line has its own current rating according to the conductor size. Assume a nominal operating system voltage V_n. The switches on both ends of a trunk line should be opened whenever

$$\frac{V_n}{\frac{Z_s}{2}+Z_p} \geq I_{\text{trunk rating}} \quad (10)$$

Conventional fault control at the distribution level focuses on current amplitude. Breakers are set to trip at a certain level. Smart breaker control attempts to reestablish the circuit to test whether the fault was intermittent. In the proposed system consider what happens if a line to ground fault occurs somewhere in trunk line 2. The inrush current in trunk lines 1 and 3 is considerable, and all neighboring lines will register a voltage drop. Note that the key parameter for computing Z_p in equations (7) and (9) is the difference between currents entering and leaving a given trunk line. When a fault occurs on trunk line 2, the large inrush current on the neighboring lines is a pass-through current. *By focusing on impedance and not current for fault control, the proposed approach avoids false trips* of neighboring lines.

4 Testing Fault Control

4.1 Passive Components

Consider the circuit shown in Fig. 5. Let the transmission line components, the balanced three-phase parallel load, and the unbalanced three-phase loads represent one trunk line section. There are three transmission section lines modeled as pi sections, 0.1 to 0.4 km long. Although the inductance, resistance, and capacitance of a real transmission line are distributed along the line, it can be modeled with reasonable accuracy as distributed R-L segments sandwiched between multiple capacitors to ground. Two generators excite this coupled system at 60 Hz. A 10 mΩ line to ground fault occurs on phase A. The transient is simulated using a Runge Kutta algorithm using Matlab Simulink©. The voltage and current are measured every 0.5 ms.

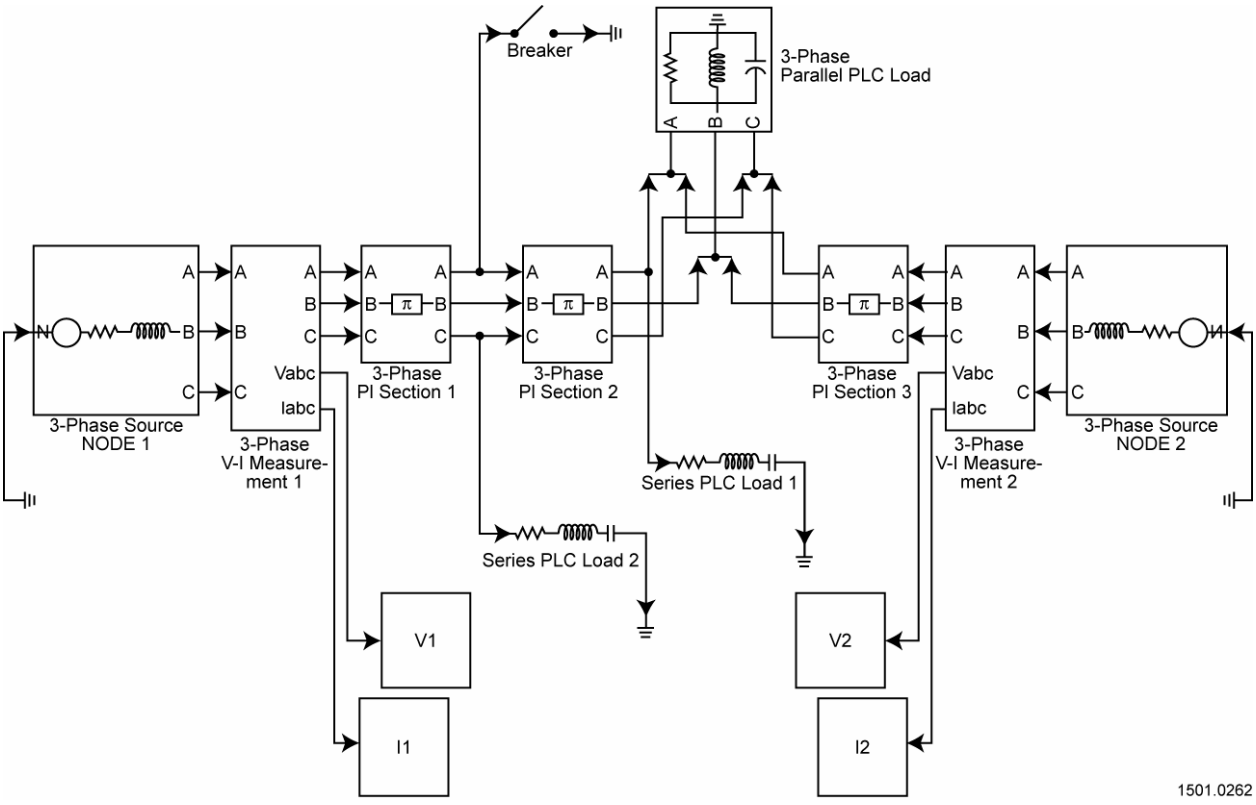

Fig. 5. Unbalanced three phase system with two generators suffering a line to phase fault.

The upper two insets of Fig. 6 show the voltage and current predicted during this event. The lower two insets show the impedances Z_s and Z_p predicted through the evaluation of Equations (8) and (9). Inductive L di/dt voltages cause the initial transient jump in voltage witnessed. Fig. 7 shows a blowup of the transient period. This simulation would suggest that about three microseconds will be required to diagnosis the fault properly. This number will be dictated by the size of the L/R components on the system.

4.2 Active Components

Consider adding a 20 kW wound rotor induction motor with a 2 mH magnetizing reactance to the model as suggested in Fig. 8. Of interest is the system performance if one phase of the motor is faulted to ground. Because of inertia the rotor will continue to rotate through the important stages of the transient introducing energy back into the grid. Because the fault is simulated five cycles into the start up cycle, the system is technically not quite in steady state equilibrium. The upper two insets of Fig. 9 show the voltage and current at node 2 simulated through the start-up transient. The lower two insets register Z_p, as calculated using equation (9). As witnessed by the previous analyses, these induction loads make the system perceive an initial increase in equivalent impedance Z_p followed by a precipitous drop. A blow-up of 2/3 of the first cycle after the fault on one leg of the induction motor is shown in Fig. 10. The additional nuance added by the induction motor is the durative aspect of the fluctuation in Z_p. The motor causes sizeable variations in Z_p through the first cycle after the fault, especially in phase. Note the considerable increase in equivalent Z_s during the fault.

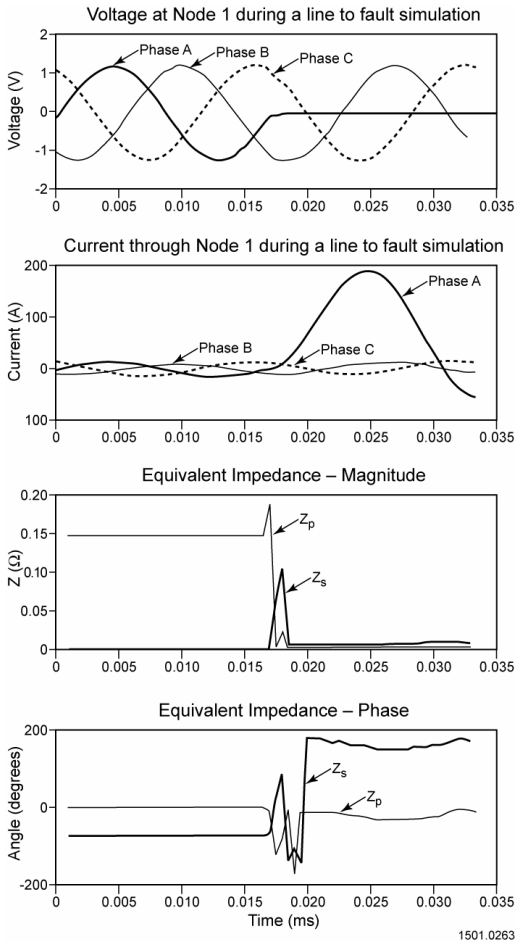

Fig. 6. Voltage, current, and impedance during a line to ground fault

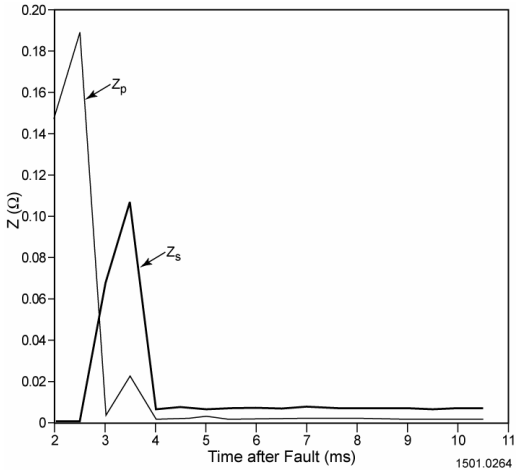

Fig. 7. Blow-up of the transient period.

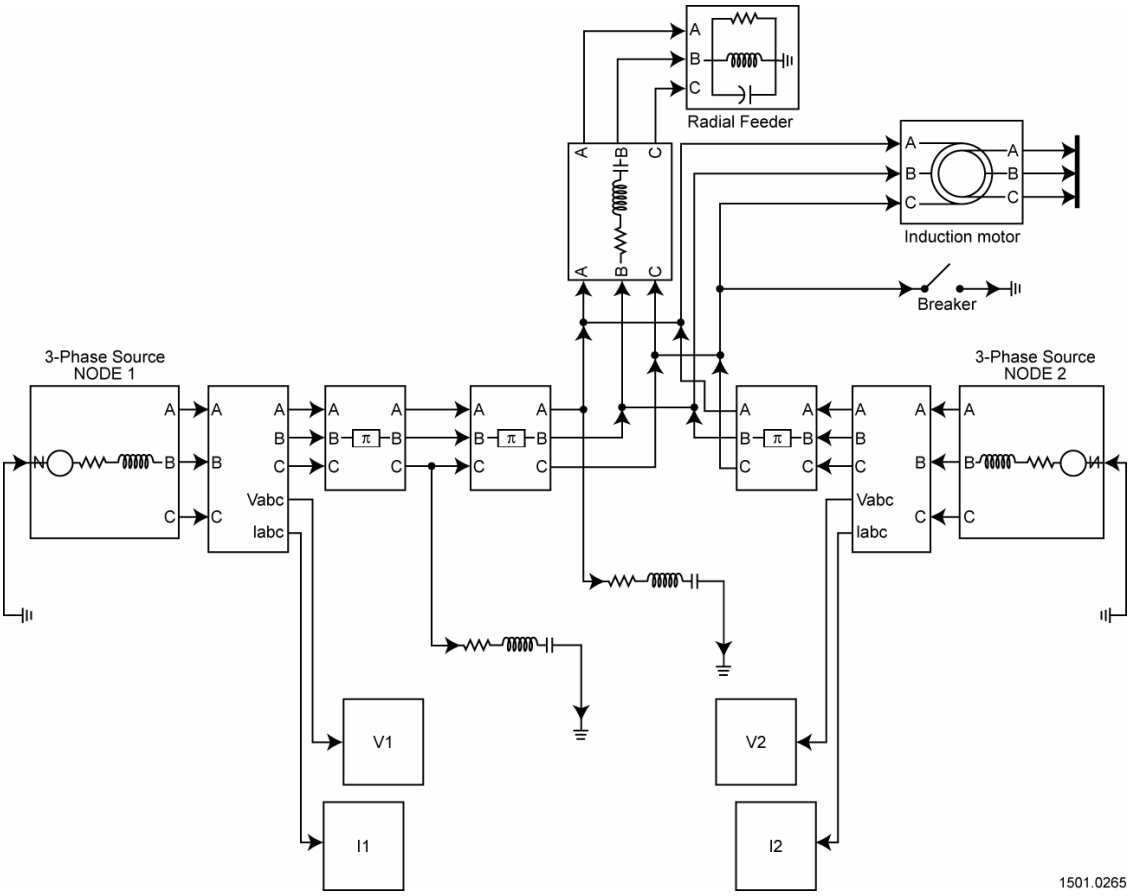

Fig. 8. Simulating a fault to a model containing a wound rotor induction motor.

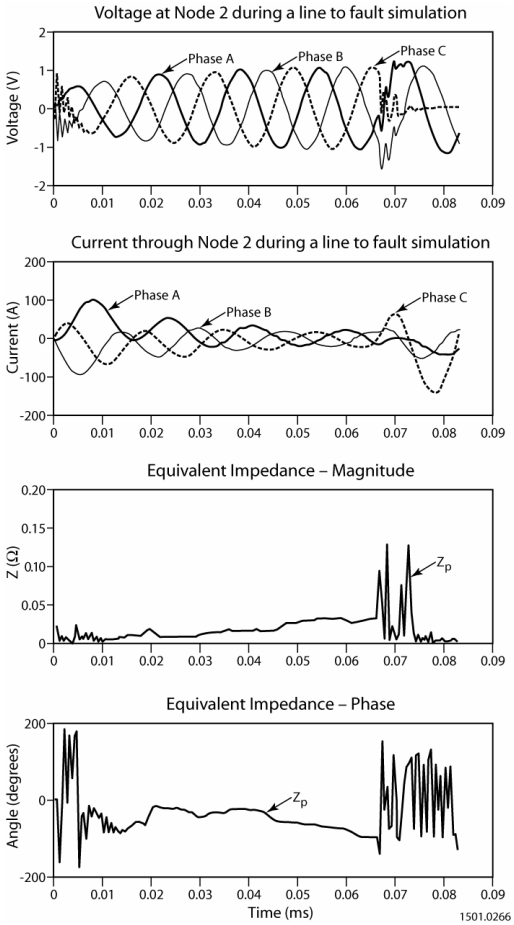

Fig. 9. Fault simulation on one phase of a three phase induction motor

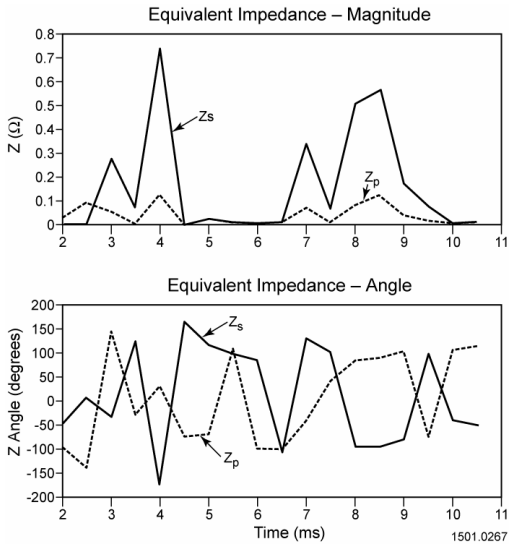

Fig. 10. Blow up of a portion of the first cycle after a fault on one leg of an induction motor

5 Conclusions

A technique is presented for quickly representing signals in terms of their phasor representation. Once accomplished, this technique allows the load over a portion of the network to be represented in terms of a series and parallel impedance. The magnitude and phase of the parallel impedance component can be used as an indicator for fault activity. Current passing through a trunk line does not alter the parallel impedance component. Careful analysis of the phase of these impedances is useful for load identification.

References

[1] S. Jiao, Z. Bo, W. Liu, and Q. Yang, "New Principles to detect faults during Power Swings," *Developments in Power System Protection Conference*, IEEE Publication No. 479, 2001, pp. 515-518.

[2] Z. Xiangjun, K. Li, W. Chan, and Y. Xianggen, "Novel Techniques for Earth Fault Feeder Detection Based on Negative Sequence Current in Industry Power Systems," *Industry Applications Conference, 2001*, Thirty-Sixth IAS Annual Meeting. Conference Record of the 2001 IEEE , Volume: 3 , 30 Sept.-4 Oct. 2001, pp. 1831 – 1837.

[3] E. Styvaktakis, I. Gu, and M. Bollen, "Voltage dip detection and power system transients," *IEEE Power Engineering Society Summer Meeting*, Volume: 1 , 15-19 July 2001, pp. 683 – 688.

[4] S. Qianli, D. Xinzhou, Z. Bo, and F. Jiang, "New approach of fault detection and fault phase selection based on initial current traveling waves," *IEEE Power Engineering Society Summer Meeting*, Volume: 1 , 21-25 July 2002, pp. 393 – 397.

[5] D. Wiot, 'A new adaptive transient monitoring scheme for detection of power system faults," *IEEE Trans. on Power System Delivery*, vol. 19, no. 1, Jan. 2004, pp. 42-48.